PHYSICAL REVIEW B **110**, L060508 (2024)

Letter | Editors' Suggestion

Zero-field finite-momentum and field-induced superconductivity in altermagnets

Debmalya Chakraborty and Annica M. Black-Schaffer
Department of Physics and Astronomy, Uppsala University, Box 516, S-751 20 Uppsala, Sweden

(Received 26 September 2023; revised 16 January 2024; accepted 24 July 2024; published 9 August 2024)

We explore the possibilities for spin-singlet superconductivity in newly discovered altermagnets. Investigating d-wave altermagnets, we show that finite-momentum superconductivity can easily emerge in altermagnets even though they have no net magnetization, when the superconducting order parameter also has d-wave symmetry with nodes coinciding with the altermagnet nodes. Additionally, we find a rich phase diagram when both altermagnetism and an external magnetic field are considered, including superconductivity appearing at high magnetic fields from a parent zero-field normal state.

DOI: 10.1103/PhysRevB.110.L060508

Introduction. Recently discovered altermagnetism [1–8] has opened up a new field of research in condensed matter physics [9] by introducing a third kind of magnetism in addition to the two long-known kinds of magnetism: ferromagnetism and antiferromagnetism. Altermagnetism appears in materials due to nonrelativistic spin splitting in the noninteracting electronic band structure and is thus not due to electronic interactions, usually associated with magnetism.

The unconventional mechanism behind altermagnetism also leads to completely different symmetry properties. In altermagnets, the magnetization appearing due to broken Kramer's spin degeneracy is momentum dependent, with sign changing values and nodes. Notably, due to the sign changes, the net magnetization is still zero in an altermagnet. Altermagnetism has already been proposed to be present in many materials with the majority of them displaying a d-wave symmetry [9], including the parent cuprate material La_2CuO_4 [3]. Since doped cuprate materials are intrinsic superconductors with spin-singlet d-wave pairing symmetry [10,11], this provides an alluring prospect of having d-wave superconductivity in altermagnets.

Almost all known superconductors are believed to be well described by Bardeen, Cooper, and Schrieffer (BCS) [12] theory, where electrons with opposite momentum k and $-k$ and opposite spins $\uparrow$ and $\downarrow$ pair in a spin-singlet configuration. These spin-singlet Cooper pairs become less energetically favorable when spin degeneracy is broken, generating a finite spin splitting due to either the application of an external magnetic field or due to the presence of intrinsic net magnetization in the material. Thus, increasing spin splitting eventually destroys the BCS state. Still, superconductivity has been shown to survive for even larger external magnetic fields, by instead forming Cooper pairs with a finite center-of-mass momentum, resulting in finite-momentum superconductivity, originally studied independently by Fulde-Ferrell (FF) [13] and Larkin-Ovchinnikov (LO) [14].

Altermagnets, due to the distinct momentum dependence of their magnetization with no net magnetization, have already been anticipated to provide intriguing possibilities for superconductivity [15]. In fact, spin-singlet Cooper pairs have very recently been studied theoretically [16–21] in altermagnets, but then only induced by the proximity effect from external superconductors, in heterostructures enticing for spintronics applications. However, despite altermagnetism being found in parent cuprate compounds, spin-singlet superconductivity as an intrinsic quantum phase of matter has not yet been explored in altermagnets.

In this Letter we investigate intrinsic superconductivity originating from an effective electron-electron attraction in d-wave altermagnetic metals. We find a highly sought-after finite-momentum superconducting phase in systems with spin-singlet d-wave superconductivity, even with no net magnetization present. However, this phase is absent in systems with spin-singlet s-wave superconductivity, which we explain by the unusual momentum-space magnetization. By also applying an external magnetic field, we also uncover a rich phase diagram resembling almost the shape of a "Yoda ear," with a cascade of phase transitions between zero- and finite-momentum pairing and normal state phases, occurring due to an intricate balance of the spin-split Fermi surface and superconducting condensation energy. Interestingly, we find a large region of field-induced superconductivity, where superconductivity only appears at high magnetic fields from a low-field normal phase. These results establish altermagnetism as a key material property for generating multiple exotic and uncommon superconducting behaviors.

Model, methods, and parameters. To capture established altermagnetism, we consider a metallic d-wave altermagnet with the Hamiltonian [3]

$$H_0 = \sum_{k,\sigma}\{\xi_k - \sigma(t_{\mathrm{am}}/2)[\cos(k_x) - \cos(k_y)] + \sigma B\}c^\dagger_{k\sigma}c_{k\sigma} + \sum_{k,k',q} V_{k,k'}c^\dagger_{k+q\uparrow}c^\dagger_{-k+q\downarrow}c_{-k'+q\downarrow}c_{k'+q\uparrow}, \quad (1)$$

where $c^\dagger_{k\sigma}$ ($c_{k\sigma}$) is the creation (annihilation) operator of an electron with spin σ and momentum k, ξ_k is the (spin-independent) electron band dispersion, and $t_{\rm am}$ is the strength of the d-wave altermagnetic spin splitting, originating from electric crystal fields. Equation (1) encodes the two bands closest to the Fermi level, thus relevant for superconductivity, in the minimal four-band lattice model of Ref. [3] [see Supplemental Material (SM) [22]. For simplicity we consider the band dispersion of a square lattice, given by $\xi_k = -2t[\cos(k_x) + \cos(k_y)] - \mu$, with $t = 1$ the nearest-neighbor hopping amplitude set as the energy unit, and μ the chemical potential tuned to fix the average density of electrons $\rho = \sum_{k,\sigma}\langle c^\dagger_{k\sigma}c_{k\sigma}\rangle$. We also include an in-plane external magnetic field B (with the electron magnetic moment $\mu_B = 1$) for controlling a Zeeman spin splitting but with no orbital effects expected. We consider intrinsic superconductivity generated by a generic effective nearest-neighbor attraction for spin-singlet pairing $V_{k,k'}$, as it is the most likely pairing [23] in the low-energy model Eq. (1),

$$V_{k,k'} = -V[\gamma(k)\gamma(k') + \eta(k)\eta(k')], \tag{2}$$

where $\gamma(k) = \cos(k_x) + \cos(k_y)$ and $\eta(k) = \cos(k_x) - \cos(k_y)$ are the two form factors for nearest-neighbor interaction on a square lattice, and V is a constant attraction strength. The nodes of the considered d-wave superconductivity lie along the $k_x = \pm k_y$ lines and matches the chosen directions of the altermagnet nodes in Eq. (1). For comparison, we also consider conventional, isotropic, s-wave pairing, using $V_{k,k'} = -V$.

We perform a mean-field decomposition of the Hamiltonian in Eq. (1) in the spin-singlet Cooper channel resulting in

$$H_{\rm MF} = \sum_{k,\sigma}\xi_{k\sigma}c^\dagger_{k\sigma}c_{k\sigma} + \sum_k\left(\Delta^Q_k c_{-k+Q/2\downarrow}c_{k+Q/2\uparrow} + \text{H.c.}\right) + \text{const}, \tag{3}$$

where now $\xi_{k\sigma} = \xi_k + \sigma(t_{\rm am}/2)[\cos(k_x) - \cos(k_y)] + \sigma B$ and Δ^Q_k is the spin-singlet superconducting order parameter obtained by the self-consistency relation

$$\Delta^Q_k = \sum_{k'}V_{k,k'}\langle c^\dagger_{k'+Q/2\uparrow}c^\dagger_{-k'+Q/2\downarrow}\rangle, \tag{4}$$

with Q being the finite center-of-mass momentum of the Cooper pair. For $t_{\rm am} = B = 0$, only zero momentum ($Q = 0$), or simply BCS pairing, is present, but due to the altermagnetism and a finite magnetic field, we always allow for a finite Q. Here, we only consider a single Q value and focus on the FF phase, where the phase of the superconducting order parameter varies but the amplitude does not [24]. Incorporating the momentum dependence of $V_{k,k'}$ in Eq. (2) we can write $\Delta^Q_k = \Delta^Q_d\eta(k) + \Delta^Q_s\gamma(k)$, with Δ^Q_d being the d-wave superconducting order parameter and Δ^Q_s being the extended s-wave superconducting order parameter [25], where both $\Delta^Q_{s,d}$ parametrically depending on Q. We solve the Hamiltonian $H_{\rm MF}$ in Eq. (3) self-consistently using Eq. (4) for fixed Q, and then obtain the true ground state by minimizing the ground state energy, $E = \sum_{k,\sigma}\xi_{k\sigma}\langle c^\dagger_{k\sigma}c_{k\sigma}\rangle - (\Delta^Q_d)^2/V - (\Delta^Q_s)^2/V + \mu\rho$, with respect to Q.

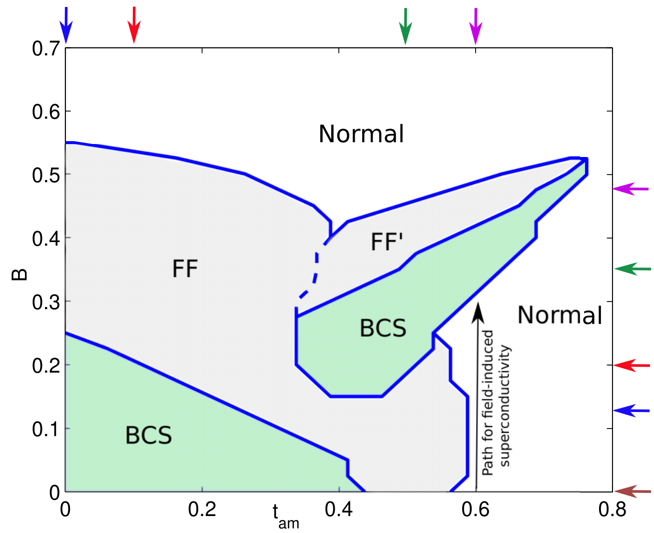

FIG. 1. Phase diagram of d-wave superconductivity in the B-$t_{\rm am}$ plane indicating a finite-momentum (FF) superconducting phase (gray), BCS zero-momentum superconductivity (green), and normal phase (white) with boundaries in between (blue lines) and between different FF phases (dashed blue line). The normal phase is identified as $\Delta^Q_d < 0.0009$ for all Q values. Calculations are performed at a set of discrete points in the B-$t_{\rm am}$ plane, spaced 0.025 apart, with blue lines drawn by taking the midpoint of the two values of $t_{\rm am}$ hosting different phases for a fixed B. The long arrow indicates one path for field-induced superconductivity, while short colored arrows indicate line cuts in Fig. 2.

In the following we report results for $V = 2$ and $\rho = 0.6$ on a square lattice of size 1000×1000, enough to mimic the thermodynamic limit and capture relevant values of Q. Other values of V and ρ give no qualitative difference (see SM [22]). Q is a vector with two possible directions in two dimensions. We show in the SM [22] that the ground state energy minima occur for a uniaxial Q along the x axis and we thus only show results for uniaxial Q, setting $Q_x \equiv Q$ for simplicity. We further find that Δ^Q_s is very small compared to Δ^Q_d for all investigated parameters, thus we only report values for Δ^Q_d.

Results. We first show in Fig. 1 the ground state phase diagram obtained by varying B and $t_{\rm am}$, for a range of realistic strengths [9]. The phase diagram broadly consists of three different phases: the BCS phase (green), finite-momentum FF phase (gray), and normal phase with no superconductivity (white). Here, we characterize the BCS phase as when the ground state energy for $Q = 0$ is the lowest, while for the FF phase a $Q \neq 0$ has the lowest energy. For comparison we report the same phase diagram for conventional s-wave superconductivity in the SM [22].

Focusing first on the situation with no applied magnetic field, $B = 0$, we find a finite-momentum FF phase for a range of finite altermagnet strengths ($0.44 \lesssim t_{\rm am} \lesssim 0.56$). This is remarkable since here the FF phase is obtained without any net magnetization in the system, in contrast to its usual occurrence in finite fields [13]. This finding is perhaps even more surprising when noting that an FF phase is absent for s-wave superconductors at zero field (see SM [22]). The emergence of a $B = 0$ FF phase in d-wave superconductors can be understood by considering the nodal structure of both the superconductor and altermagnet [see Fig. 3(a)]. Since the nodes for both the altermagnet (where there is no spin splitting) and the d-wave superconducting order parameter (where the order parameter is zero) lie along the $k_x = \pm k_y$ lines, the gapped parts of the Fermi surface, with a finite superconducting order parameter, always host a finite magnetization due to the altermagnetism. As a result, electrons with $k, \uparrow$ only finds their spin-singlet BCS Cooper partners $-k, \downarrow$ at different energies due to the finite spin splitting, while pairing $k, \uparrow$ and $-k + Q, \downarrow$ can still occur at the zero-energy difference, thus resulting in a finite Q FF ground state. In contrast, s-wave superconductors have no superconducting nodes and the system can then still gain sufficient condensation energy by forming zero-momentum BCS pairs around the altermagnet nodal points, where the Fermi surface retains its spin degeneracy, thus preventing an FF ground state.

Next, considering the $t_{\rm am} = 0$ line, we find the well-established transitions of BCS to FF to normal phases with increasing B [13], but with increasing $t_{\rm am}$ and finite $B \neq 0$ this drastically changes and we uncover an interesting phase diagram looking a bit like a "Yoda ear." For weak $t_{\rm am} \lesssim 0.34$, transitions are similar to $t_{\rm am} = 0$, though with increasing $t_{\rm am}$, the critical B required for the BCS to FF transition is reduced, eventually reaching zero for $t_{\rm am} \approx 0.44$ as discussed above. However, for $t_{\rm am} \gtrsim 0.34$, the BCS phase reappears at higher B, thus generating a cascade of phase transitions. For example, in the regime $0.44 \lesssim t_{\rm am} \lesssim 0.56$, the system shows three different transitions with increasing B: one from FF to BCS, the next from BCS to another FF′ phase, and eventually from the FF′ phase to the normal phase. The large-B FF′ phase is characterized as a different FF phase due to a distinctly different Q vector, as detailed below. Another remarkable feature occurs for $0.59 \lesssim t_{\rm am} \lesssim 0.76$. In this regime of altermagnetism, the system is in a normal phase at zero magnetic field $B = 0$, but then superconductivity emerges with increasing magnetic field, first by forming a BCS phase and then transitioning into the FF′ phase. In Fig. 1 we illustrate one such path of field-induced superconductivity. Field-induced superconductivity should be impossible in spin-singlet superconductors, but here the altermagnetism provides a route to still generate it.

In order to understand superconductivity within each individual phase, we show in Fig. 2 the superconducting order parameter Δ_d^Q [Figs. 2(a) and 2(b)] and Q values [Figs. 2(c) and 2(d)] in the ground state for different line cuts of the phase diagram in Fig. 1, indicated by color arrows and chosen to capture all distinct phase transitions. In Figs. 2(a) and 2(c), we show five different line cuts for fixed B values, varying $t_{\rm am}$. For $B = 0$ (brown dot), Q becomes finite in the region $0.44 \lesssim t_{\rm am} \lesssim 0.56$, capturing the FF phase even in the absence of applied field. The corresponding Δ_d^Q displays an expected jump [13] from the BCS value to a lower value in the FF phase and with a further reduction toward zero with increasing $t_{\rm am}$. For a higher $B = 0.12$ (blue plus), the FF phase is found over an even wider range of $t_{\rm am}$, with a notable monotonic increase in Q. Here, the jump in Δ_d^Q from the BCS value to the FF value is notably suppressed. Further increasing the magnetic field to $B = 0.2$ (red star) results in four transitions as $t_{\rm am}$ is

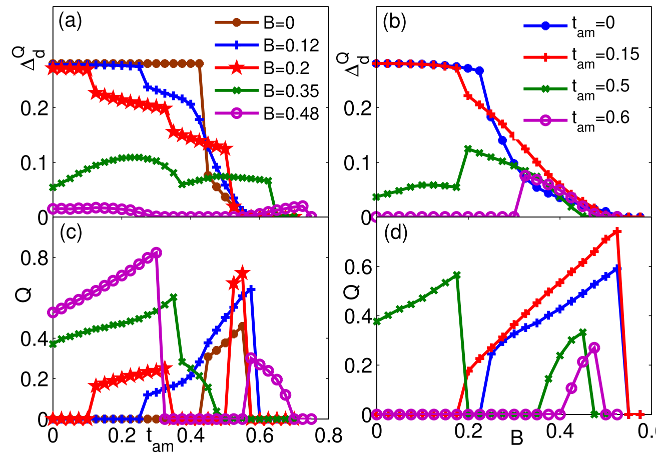

FIG. 2. Superconducting order parameter Δ_d^Q [(a), (b)] and values of Q [(c), (d)] in different ground states (lowest total energy) at fixed values of B, varying $t_{\rm am}$ [(a), (c)] and fixed values of $t_{\rm am}$, varying B [(b), (d)].

increased: BCS to FF, FF to BCS, BCS to FF, and eventually FF to the normal phase, with both Q and Δ_d^Q displaying jumps between BCS to FF or FF to BCS transitions. The difference in Q values of the two FF phases separated by the intermediary BCS phase can be thought of as reminiscent of the notable monotonic increase in Q in the FF phase for lower B (compare the blue plus and red star curves). For $B = 0.35$ (green cross), the system instead goes from one FF phase directly to another FF′ phase with increasing $t_{\rm am}$, with a distinct jump in Q values at the transition. As we establish in the SM [22], this is due to two competing FF states with different $Q \neq 0$ in this regime of B. The global energy minima is obtained for one Q for a range of $t_{\rm am}$ and then the energy balance shifts to the other Q at higher $t_{\rm am}$. With an even further increase in $t_{\rm am}$, the $Q = 0$ solution becomes most energetically favorable, before eventually reaching the normal phase at large $t_{\rm am}$. Due to this competition between different local energy minima, Δ_d^Q shows a nonmonotonic behavior with increasing $t_{\rm am}$ and is also suppressed at the FF to FF′ transition. This suppression is enhanced for larger B, eventually reducing Δ_d^Q to zero resulting in a normal phase between two FF phases, as seen for $B = 0.48$ (magenta circle).

The field behavior including field-induced superconductivity is most prominent in line cuts at fixed $t_{\rm am}$ and varying B, as shown in Figs. 2(b) and 2(d). For $t_{\rm am} = 0.0, 0.15$ (blue dot, red plus), Δ_d^Q and Q shows behavior expected in a spin-singlet superconductor in an applied magnetic field, with the BCS phase giving way to the FF phase at larger fields [13]. Here, larger $t_{\rm am}$ makes the FF phase occurring in a larger parameter space. For $t_{\rm am} = 0.5$ (green cross) the situation is notably changed. At zero and low fields an FF phase is present, which then transitions into a BCS phase at finite fields, a transition that is accompanied with a notably large increase in Δ_d^Q. Thus an applied magnetic field here causes a strengthening of superconductivity. Beyond the BCS phase, another FF′ phase appears, before transitioning into the normal phase. Finally, at higher $t_{\rm am} = 0.6$ (magenta circle), Δ_d^Q instead clearly jumps from zero to a finite value with

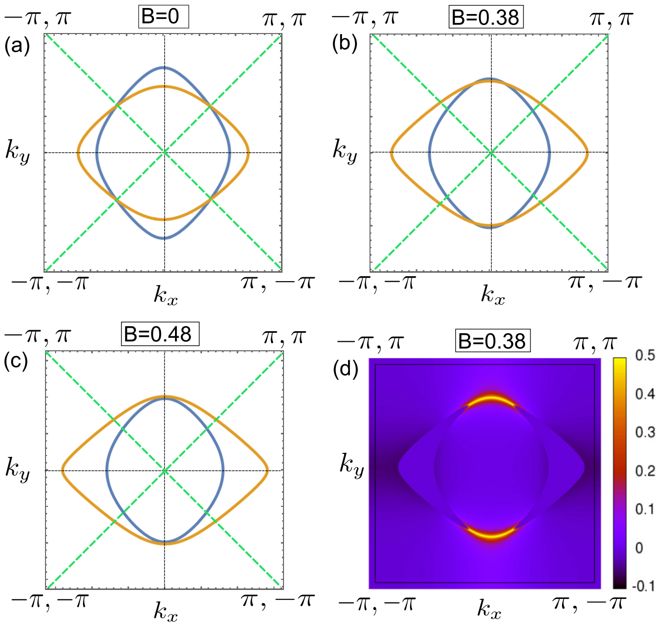

FIG. 3. (a)–(c) Contour plots of the normal state electronic bands $\xi_{k\uparrow} = 0$ (yellow) and $\xi_{k\downarrow} = 0$ (blue) signifying the spin-split Fermi surfaces present at $t_{\text{am}} = 0.6$. The dashed green lines mark the d-wave superconducting order parameter nodes. (d) Pair density $\langle c_k^\dagger c_{-k}^\dagger \rangle$.

increasing magnetic field, showing the emergence of field-induced superconductivity.

The remarkable finding of field-induced superconductivity can be understood by looking at the normal state band structures. For clarity we focus on the field-induced path marked in Fig. 1 and show in Fig. 3 the normal state Fermi surface of opposite spins for increasing B at fixed $t_{\text{am}} = 0.6$. For $B = 0$ in Fig. 3(a), the Fermi surfaces of $\uparrow$-spin (yellow) and $\downarrow$-spin (blue) are split significantly, especially in regions away from the superconducting nodes (dashed green), implying that $k, \uparrow$ and $-k, \downarrow$ electrons are far apart in energy in these regions. Consequently, spin-singlet pairing is energetically unfavorable, which explains the lack of zero-field superconductivity. As shown in Fig. 3(b), increasing the magnetic field to $B = 0.38$ compensates the spin splitting due to altermagnetism on some parts of the Fermi surface. This feature is related to a topological nodal to nodeless transition in altermagnets [26]. In particular, regions of the Fermi surface near $k_x = 0$ have now almost no spin splitting and spin-singlet zero-momentum BCS pairing can thus be realized here [see the pair density plot in Fig. 3(d)]. Notably, finite B makes the Fermi surfaces asymmetric between $k_y = 0$ and $k_x = 0$, with parts near $k_y = 0$ regions still showing notable spin splitting. Now, since a d-wave superconducting gap has maxima in its antinodal regions (i.e., around the $k_{x,y} = 0$ regions), a finite condensation energy is possible by producing spin-singlet pairing near the $k_x = 0$ regions. In contrast, for s-wave superconductors the gap is isotropic and thus the condensation energy gain with pairing only around the $k_x = 0$ regions does not stabilize s-wave superconductivity. This makes field-induced s-wave superconductivity absent in the s-wave superconductivity phase diagram (see SM [22]). A further increase in magnetic field to $B = 0.48$ in Fig. 3(c) results in a separation of the two spin Fermi surfaces also in the $k_x = 0$ regions. Subsequently, BCS pairing becomes unstable and finite-momentum FF′ pairing occurs instead, before eventually, for even stronger B, the spin splitting is significant for all momenta and all types of superconductivity is destroyed.

Discussion. Considering spin-singlet superconductivity in altermagnets we find a finite-momentum (FF) superconducting phase in the absence of an applied magnetic field. This zero-field FF phase is dependent on coinciding superconducting gap and altermagnet nodes, and do not appear in an s-wave superconductor. In the presence of external magnetic field, we also uncover field-induced superconductivity, due to an intricate interplay between the Fermi surface shape and superconducting condensation energy. Although we are primarily concerned with d-wave symmetry, our results are also directly applicable to g- and i-wave altermagnets, as long as the superconducting pairing at least partially has the same nodal structure (see SM [22]). We further validate that our finding of a zero-field FF phase is robust and present also when altermagnetism is induced by interactions [27] (see SM).

Our finding of zero-field finite-momentum superconductivity is remarkable since the net magnetization is always zero in altermagnets. Finding finite-momentum superconductivity in microscopic models in the absence of applied magnetic field has been a long-standing unsolved theory problem [28–31], despite mounting experimental evidence of such a phase, often referred to as pair density waves [32–39]. Our work provides one straightforward path to realize finite-momentum superconductivity likely applicable to many materials, including the possibility of being the origin of such a phase in the cuprate superconductors, without needing the preceding charge density order [31,33,40–44]. Moreover, finite-momentum superconductivity may be important for technological applications, as, e.g., illustrated by superconducting diode effects [45–47], opening up a large technological potential for superconducting altermagnets. Another remarkable feature of our results is the presence of a field-induced superconducting phase at experimentally accessible fields (see SM [22]). Such a phase is both rare [48–50] and unexpected, but has gained renewed interest after its recent observation in UTe_2 [51]. Our work also opens many other exotic possibilities of superconductivity. Investigating the relation of the finite-momentum Cooper pairs in altermagnets and odd-frequency pairing, or generally finite-energy pairs, is one interesting direction [52–54]. The additional presence of relativistic spin-orbit coupling can further provide a platform for studying the interplay of finite-momentum and topological superconductivity [55,56].

Although superconductivity has not yet been discovered experimentally in altermagnetic materials within the two years of their discovery, our results point out several promising directions. With too large altermagnetic spin splitting only the normal phase is reached and thus limiting altermagnetism is favorable. Or, for strong altermagnetism, applying an external magnetic field can be used to induce superconductivity. Moreover, d-wave superconductivity is likely much more amenable to altermagnetism than conventional s-wave superconductivity. Alternatively, doping altermagnet insulators, making them metallic, is also a promising route.

Note added. Recently, we became aware of Refs. [57,58], where a zero-field finite-momentum phase is discussed in the context of cuprates with nematic–spin-nematic order and organic conductors with antiferromagnetism, respectively.

Acknowledgments. We gratefully acknowledge financial support from the Knut and Alice Wallenberg Foundation through the Wallenberg Academy Fellows program, KAW 2019.0309, and the Swedish Research Council (Vetenskapsrådet) Grant Agreement No. 2022-03963. The computations were enabled by resources provided by the National Academic Infrastructure for Supercomputing in Sweden (NAISS) at the Uppsala Multidisciplinary Center for Advanced Computational Science (UPPMAX) funded by the Swedish Research Council through Grant Agreement No. 2022-06725.

[1] L. Šmejkal, R. González-Hernández, T. Jungwirth, and J. Sinova, Sci. Adv. **6**, eaaz8809 (2020).
[2] I. I. Mazin, K. Koepernik, M. D. Johannes, R. González-Hernández, and L. Šmejkal, Proc. Natl. Acad. Sci. USA **118**, e2108924118 (2021).
[3] L. Šmejkal, J. Sinova, and T. Jungwirth, Phys. Rev. X **12**, 031042 (2022).
[4] Z. Feng, X. Zhou, L. Šmejkal, L. Wu, Z. Zhu, H. Guo, R. González-Hernández, X. Wang, H. Yan, P. Qin, X. Zhang, H. Wu, H. Chen, Z. Meng, L. Liu, Z. Xia, J. Sinova, T. Jungwirth, and Z. Liu, Nat. Electron. **5**, 735 (2022).
[5] S. Hayami, Y. Yanagi, and H. Kusunose, J. Phys. Soc. Jpn. **88**, 123702 (2019).
[6] S. Hayami, Y. Yanagi, and H. Kusunose, Phys. Rev. B **102**, 144441 (2020).
[7] R. D. G. Betancourt, J. Zubáč, R. Gonzalez-Hernandez, K. Geishendorf, Z. Šobáň, G. Springholz, K. Olejník, L. Šmejkal, J. Sinova, T. Jungwirth, S. T. B. Goennenwein, A. Thomas, H. Reichlová, J. Železný, and D. Kriegner, Phys. Rev. Lett. **130**, 036702 (2023).
[8] H. Bai, Y. C. Zhang, Y. J. Zhou, P. Chen, C. H. Wan, L. Han, W. X. Zhu, S. X. Liang, Y. C. Su, X. F. Han, F. Pan, and C. Song, Phys. Rev. Lett. **130**, 216701 (2023).
[9] L. Šmejkal, J. Sinova, and T. Jungwirth, Phys. Rev. X **12**, 040501 (2022).
[10] D. Scalapino, Phys. Rep. **250**, 329 (1995).
[11] C. C. Tsuei and J. R. Kirtley, Rev. Mod. Phys. **72**, 969 (2000).
[12] J. Bardeen, L. N. Cooper, and J. R. Schrieffer, Phys. Rev. **108**, 1175 (1957).
[13] P. Fulde and R. A. Ferrell, Phys. Rev. **135**, A550 (1964).
[14] A. I. Larkin and Y. N. Ovchinnikov, Zh. Eksp. Teor. Fiz. **47**, 1136 (1964).
[15] I. I. Mazin, arXiv:2203.05000.
[16] S.-B. Zhang, L.-H. Hu, and T. Neupert, Nat. Commun. **15**, 1801 (2024).
[17] M. Wei, L. Xiang, F. Xu, L. Zhang, G. Tang, and J. Wang, Phys. Rev. B **109**, L201404 (2024).
[18] J. A. Ouassou, A. Brataas, and J. Linder, Phys. Rev. Lett. **131**, 076003 (2023).
[19] C. W. J. Beenakker and T. Vakhtel, Phys. Rev. B **108**, 075425 (2023).
[20] M. Papaj, Phys. Rev. B **108**, L060508 (2023).
[21] H. G. Giil and J. Linder, Phys. Rev. B **109**, 134511 (2024).
[22] See Supplemental Material at http://link.aps.org/supplemental/10.1103/PhysRevB.110.L060508 for the equivalence of the low-energy two-band model considered in the main text with the four-band model proposed in Ref. [3], the phase diagram for s-wave superconductivity, the ground state energy in full (Q_x, Q_y) space, representative line cuts to illustrate phase transitions between different Q values, the d-wave phase diagram for smaller interaction strength, results for a different, interaction-driven, model of altermagnetism, and which includes Refs. [59,60].
[23] D. Chakraborty and A. M. Black-Schaffer (unpublished).
[24] We do not consider the LO phase due to the additional complexity of related charge density waves [61], as already the FF phase shows that finite-momentum pairing is favorable. The total current of the FF phase is still zero, despite the finite Q [13].
[25] K. Fossheim and A. Sudbø, *Superconductivity: Physics and Applications* (Wiley, Hoboken, NJ, 2005).
[26] R. M. Fernandes, V. S. de Carvalho, T. Birol, and R. G. Pereira, Phys. Rev. B **109**, 024404 (2024).
[27] T. A. Maier and S. Okamoto, Phys. Rev. B **108**, L100402 (2023).
[28] H. Chen and H.-J. Gao, Nature (London) **618**, 910 (2023).
[29] Y.-M. Wu, P. A. Nosov, A. A. Patel, and S. Raghu, Phys. Rev. Lett. **130**, 026001 (2023).
[30] K. S. Huang, Z. Han, S. A. Kivelson, and H. Yao, npj Quantum Mater. **7**, 17 (2022).
[31] D. F. Agterberg, J. S. Davis, S. D. Edkins, E. Fradkin, D. J. Van Harlingen, S. A. Kivelson, P. A. Lee, L. Radzihovsky, J. M. Tranquada, and Y. Wang, Annu. Rev. Condens. Matter Phys. **11**, 231 (2020).
[32] M. H. Hamidian, S. D. Edkins, S. H. Joo, A. Kostin, H. Eisaki, S. Uchida, M. J. Lawler, E.-A. Kim, A. P. Mackenzie, K. Fujita, J. Lee, and J. C. S. Davis, Nature (London) **532**, 343 (2016).
[33] S. D. Edkins, A. Kostin, K. Fujita, A. P. Mackenzie, H. Eisaki, S. Uchida, S. Sachdev, M. J. Lawler, E.-A. Kim, J. C. Séamus Davis, and M. H. Hamidian, Science **364**, 976 (2019).
[34] X. Liu, Y. X. Chong, R. Sharma, and J. C. S. Davis, Science **372**, 1447 (2021).
[35] S. Kasahara, Y. Sato, S. Licciardello, M. Čulo, S. Arsenijević, T. Ottenbros, T. Tominaga, J. Böker, I. Eremin, T. Shibauchi, J. Wosnitza, N. E. Hussey, and Y. Matsuda, Phys. Rev. Lett. **124**, 107001 (2020).
[36] H. Chen, H. Yang, B. Hu, Z. Zhao, J. Yuan, Y. Xing, G. Qian, Z. Huang, G. Li, Y. Ye, S. Ma, S. Ni, H. Zhang, Q. Yin, C. Gong, Z. Tu, H. Lei, H. Tan, S. Zhou, C. Shen *et al.*, Nature (London) **599**, 222 (2021).
[37] Q. Gu, J. P. Carroll, S. Wang, S. Ran, C. Broyles, H. Siddiquee, N. P. Butch, S. R. Saha, J. Paglione, J. C. S. Davis, and X. Liu, Nature (London) **618**, 921 (2023).
[38] Y. Liu, T. Wei, G. He, Y. Zhang, Z. Wang, and J. Wang, Nature (London) **618**, 934 (2023).
[39] H. Zhao, R. Blackwell, M. Thinel, T. Handa, S. Ishida, X. Zhu, A. Iyo, H. Eisaki, A. N. Pasupathy, and K. Fujita, Nature (London) **618**, 940 (2023).

[40] Z. Dai, Y.-H. Zhang, T. Senthil, and P. A. Lee, Phys. Rev. B **97**, 174511 (2018).
[41] Z. Dai, T. Senthil, and P. A. Lee, Phys. Rev. B **101**, 064502 (2020).
[42] P. A. Lee, Phys. Rev. X **4**, 031017 (2014).
[43] M. R. Norman and J. C. S. Davis, Proc. Natl. Acad. Sci. USA **115**, 5389 (2018).
[44] D. Chakraborty, M. Grandadam, M. H. Hamidian, J. C. S. Davis, Y. Sidis, and C. Pépin, Phys. Rev. B **100**, 224511 (2019).
[45] F. Ando, Y. Miyasaka, T. Li, J. Ishizuka, T. Arakawa, Y. Shiota, T. Moriyama, Y. Yanase, and T. Ono, Nature (London) **584**, 373 (2020).
[46] A. Daido, Y. Ikeda, and Y. Yanase, Phys. Rev. Lett. **128**, 037001 (2022).
[47] N. F. Q. Yuan and L. Fu, Proc. Natl. Acad. Sci. USA **119**, e2119548119 (2022).
[48] H. W. Meul, C. Rossel, M. Decroux, O. Fischer, G. Remenyi, and A. Briggs, Phys. Rev. Lett. **53**, 497 (1984).
[49] S. Uji, H. Shinagawa, T. Terashima, T. Yakabe, Y. Terai, M. Tokumoto, A. Kobayashi, H. Tanaka, and H. Kobayashi, Nature (London) **410**, 908 (2001).
[50] T. Konoike, S. Uji, T. Terashima, M. Nishimura, S. Yasuzuka, K. Enomoto, H. Fujiwara, B. Zhang, and H. Kobayashi, Phys. Rev. B **70**, 094514 (2004).
[51] S. Ran, I.-L. Liu, Y. S. Eo, D. J. Campbell, P. M. Neves, W. T. Fuhrman, S. R. Saha, C. Eckberg, H. Kim, D. Graf, F. Balakirev, J. Singleton, J. Paglione, and N. P. Butch, Nat. Phys. **15**, 1250 (2019).
[52] D. Chakraborty and A. M. Black-Schaffer, New J. Phys. **23**, 033001 (2021).
[53] D. Chakraborty and A. M. Black-Schaffer, Phys. Rev. Lett. **129**, 247001 (2022).
[54] D. Chakraborty and A. M. Black-Schaffer, Phys. Rev. B **106**, 024511 (2022).
[55] D. Zhu, Z.-Y. Zhuang, Z. Wu, and Z. Yan, Phys. Rev. B **108**, 184505 (2023).
[56] S. A. A. Ghorashi, T. L. Hughes, and J. Cano, arXiv:2306.09413.
[57] R. Soto-Garrido and E. Fradkin, Phys. Rev. B **89**, 165126 (2014).
[58] S. Sumita, M. Naka, and H. Seo, Phys. Rev. Res. **5**, 043171 (2023).
[59] T. Nagamiya, K. Yosida, and R. Kubo,, Adv. Phys. **4**, 1 (1955).
[60] A. N. Bogdanov, A. V. Zhuravlev, and U. K. Rößler, Phys. Rev. B **75**, 094425 (2007).
[61] A. Datta, K. Yang, and A. Ghosal, Phys. Rev. B **100**, 035114 (2019).